Applied Catalysis A: General 522 (2016) 45–53

Contents lists available at ScienceDirect

Applied Catalysis A: General

journal homepage: www.elsevier.com/locate/apcata

Conversion of benzyl alcohol to benzonitrile over a $Cu_{10.3}/SiO_2$ catalyst

Yuecheng Zhang, Xiaofu Zhao, Hongyu Zhang, Xiang Yan, Jiquan Zhao*

School of Chemical Engineering and Technology, Hebei University of Technology, Tianjin 300130, PR China

ARTICLE INFO

Article history:
Received 18 January 2016
Received in revised form 27 April 2016
Accepted 27 April 2016
Available online 28 April 2016

Keywords:
Benzonitrile
Benzyl alcohol
Amination-dehydrogenation
Ammonia

ABSTRACT

A $Cu_{10.3}/SiO_2$ catalyst was prepared for the conversion of benzyl alcohol to benzonitrile through amination-dehydrogenation process. The catalyst showed high activity in the reaction, and a yield as high as 98.0% was reached under the optimized conditions. The catalyst was characterized by XRD, TEM-EDX, TG-DSC, N_2 adsorption-desorption and IR of absorbed pyridine methods. The characterization results disclosed that the doping of copper created Lewis acid sites in the matrix of SiO_2. The doped copper in the fresh catalyst was present in CuO state, which was reduced to elemental Cu by H_2 generated in situ in the catalytic run. The characterization results also disclosed that the catalyst deactivation was mainly caused by the carbonaceous deposition on the surface of the catalyst in the catalytic reaction. The experimental results confirmed that most activity of the catalyst can be recovered at 550 °C online by blowing air into the reactor. Partial sintering of copper particles took place during the catalytic run, which led to the slight decreases of Lewis acidity and dehydrogenation capacity, therefore, caused deviation of the performance of the regenerated $Cu_{10.3}/SiO_2$ catalyst from that of the fresh one.

1. Introduction

Benzonitrile is an aprotic polar molecule with a dipole moment of 4.18 D, and for this reason it has been extensively used in chemistry as solvent [1–4], and now is also used in dye sensitized solar cells [5,6]. As other applications, benzonitrile is useful as a starting material in production of plastics, pharmaceuticals, surface-active compounds, synthetic dyes and so on [7–9].

Benzonitrile is generally manufactured by ammoxidation of toluene catalyzed by various catalysts (Eq. (1)) [10–15].

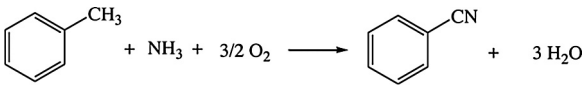

(1)

However, traces amount of hydrogen cyanide is generally generated in ammoxidation, which causes environmental pollution in the production process. The other methods for synthesizing benzonitrile involve direct condensation of hydrogen cyanide with benzene (Eq. (2)) [16,17], and cyanation of diazobenzene or phenyl halides using cuprous cyanide or other salts of hydrogen cyanide as cyano sources (Eq. (3)) [18–21].

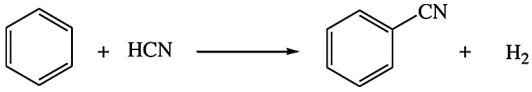

(2)

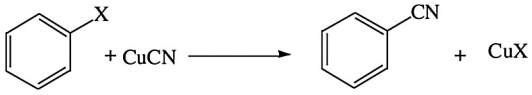

(3)

X = F, Cl, Br, I, N_2Cl

In these cases highly toxic hydrogen cyanide and its salts are employed as starting materials, therefore, it is not recommendable from the viewpoint of green chemistry. On the other hand aliphatic nitriles, such as acetonitrile, can be synthesized from alcohols by two approaches: amination-dehydrogenation [22,23] and ammoxidation [24–26]. In the amination—dehydrogenation process, two moles of hydrogen are released as shown in Eq. (4):

$$RCH_2OH + NH_3 \rightarrow RCN + H_2O + 2H_2 \quad (4)$$

Compared to ammoxidation process this process has the advantage of without formation of hydrogen cyanide due to no oxygen participation in the reaction. Meanwhile, the H_2 formed as by-product can be easily separated by pressure swing adsorption (PSA) process and compressed as a product. Therefore this process can be regarded as a green and safe technology.

* Corresponding author.
E-mail address: zhaojq@hebut.edu.cn (J. Zhao).

http://dx.doi.org/10.1016/j.apcata.2016.04.031
0926-860X/

In recent years, we successfully synthesized aliphatic nitriles through the amination—dehydrogenation of corresponding alcohols [23,27–29] over a CoNi/γ-Al_2O_3 catalyst; we also succeeded in obtaining a ZnCr/γ-Al_2O_3 catalyst being active in the synthesis of phenylacetonitrile [30] and propionitrile [31] from styrene oxide and allyl alcohol through the amination—dehydrogenation, respectively. Based on the CoNi/γ-Al_2O_3 catalyst and the parameters obtained in laboratory, acetonitrile can be produced on a pilot scale from ethanol by us. Encouraged by the results we are engaged in the synthesis of benzonitrile from the amination-dehydrogenation of benzyl alcohol. A series of catalysts have been prepared and it has been found that a $Cu_{10.3}/SiO_2$ catalyst is very efficient in the conversion of benzyl alcohol to benzonitrile. Herein, we report the results.

2. Experimental

2.1. Catalyst preparation

The metal nitrates $Cu(NO_3)_2{\cdot}3H_2O$ (99%), $Fe(NO_3)_2{\cdot}9H_2O$ (98.5%), $Co(NO_3)_2{\cdot}6H_2O$ (99%), $Ni(NO_3)_2{\cdot}6H_2O$ (98%), $Zn(NO_3)_2{\cdot}6H_2O$ (99%), $Cr(NO_3)_3{\cdot}9H_2O$ (99%), $Ca(NO_3)_2{\cdot}4H_2O$ (99%), $Na_2SiO_3{\cdot}9H_2O$ (Na_2O 22.8-23.5%, Na_2O: SiO_2 = 1.03) and other reagents used for preparation of the catalysts were obtained from KRS Chemical Reagent Cooperation, Tianjin, China. The mordenite, H-ZSM-5 and sodium bentonite were acquired from Nankai University Catalyst Plant, Tianjin, China. TiO_2 and γ-Al_2O_3 were obtained from the Tianjin Research and Design Institute of Chemical Industry, Tianjin, China.

Series of catalysts with different metal contents on various supports were prepared, which was denoted as M_x/S, where M, $_x$ and S represent the type of transition metal, the metal content in the catalyst and the type of support, respectively. Thus, the Cu/SiO_2 catalysts were denoted as Cu_x/SiO_2, where $_x$ represents the copper content in the catalyst.

H_2SiO_3 was employed as the precursor of SiO_2 and prepared as follows: 85.09 g of $Na_2SiO_3{\cdot}9H_2O$ was dissolved in 198.55 g of distilled water, then 30% (v/v) nitric acid was dropped slowly into this solution under mechanical stirring at 40 °C until the pH reached 5. The reaction mixture was stirred for 1 h, then filtered, and the solid was washed with distilled water thoroughly until the pH of the filtrate reached 7. Then the solid was dried at 110 °C for 3 h to obtain the H_2SiO_3.

The Cu/SiO_2 catalysts were prepared by kneading a mixture of H_2SiO_3 with an aqueous solution of the corresponding transition-metal nitrates, then extruded, dried and calcined. As an example, the $Cu_{10.3}/SiO_2$ catalyst was prepared as the following procedures: 7.6 g of $Cu(NO_3)_2{\cdot}3H_2O$ was added in a beaker, and a suitable amount of distilled water was added to dissolve the nitrate, then 23.37 g of H_2SiO_3 was added to the solution. The mixture was kneaded for 3 h in a kneader and the resulting kneaded material was processed in an extruder to obtain extrudates with a diameter of 2 mm and a length of 2.5 mm. The catalyst precursor was dried at 110 °C for 6 h and calcined at 550 °C for 6 h to yield the catalyst.

The catalysts with supports except for SiO_2 and HZSM-5 were prepared by the impregnation- kneading-extruding method. As an example, the $Cu_{10.2}/$γ-Al_2O_3 catalyst was prepared as the following procedures: 7.6 g of $Cu(NO_3)_2{\cdot}3H_2O$ was added in a beaker, and a suitable amount of distilled water was added to dissolve the nitrate, then 18 g of γ-Al_2O_3 was added to the solution. The mixture was kneaded for 3 h in a kneader and the resulting kneaded material was processed in an extruder to obtain extrudates with a diameter of 2 mm and a length of 2.5 mm. The catalyst precursor was dried at 110 °C for 6 h and calcined at 550 °C for 6 h to yield the catalyst.

The $Cu_{9.9}$/HZSM-5 catalyst was prepared by the impregnation method. 7.6 g of $Cu(NO_3)_2{\cdot}3H_2O$ was dissolved in 10.4 g of water, and then 18 g of HZSM-5 with a diameter of 2 mm and a length of 2.5 mm was introduced into the solution. The mixture was vigorously stirred at room temperature for 48 h and then dried at 110 °C for 6 h and calcined at 550 °C for 6 h to obtain the catalyst.

2.2. Catalyst characterization

The metal content of the catalyst samples was determined by a Perkin Elmer Opfima 7300 V type ICP-AES instrument. Before analysis, the accurately weighed sample was carefully added in a flask, and then aqua regia (HNO_3–HCl) and HF were added successively to dissolve the sample. The obtained solution was subjected for analysis.

The X-ray diffraction (XRD) patterns of the samples were recorded with a Bruker AXS GMBH D8 FOCUS X-ray diffractometer using Cu Kα radiation (40 kV, 40 mA) in the range 2θ = 10–90°. Transmission electron microscopy (TEM) was performed using a using a JEM 2100F instrument which was equipped with an energy dispersive X-ray (EDX) detector at an accelerating voltage of 200 kV. The specimens for TEM analysis were prepared by ultrasonic dispersion in ethanol, and then a drop of the resultant suspension was evaporated on a lacey carbon/Mo grid.

The surface areas, total pore volumes and pore sizes of the samples were measured at 77 K by nitrogen adsorption using a Micromeritics ASAP 2020 M + C Surface Area and Porosity Analyzer.

The IR spectra of adsorbed pyridine were recorded by a Thermo Electron Corporation Nicolet Nexus 470 spectrometer equipped with a heatable and evacuatable IR cell with CaF_2 windows connected to a gas dosing-evacuation system. The powdered samples were pressed into self-supporting wafers with a diameter of 20 mm and weight of 15 mg. Prior to analysis, all samples were pretreated at 400 °C for 1 h under high vacuum conditions (1×10^{-5} Pa), followed by cooling to 200 °C. Then pyridine was adsorbed at this temperature for 15 min. The physisorbed pyridine was removed by evacuating at 200 °C for 15 min under high vacuum conditions (1×10^{-5} Pa). Then the infrared spectra were recorded.

Thermogravimetric-different scanning calorimetry (TG-DSC) measurement was carried out with a DuPont TA2000 thermogravimetric analyser from 20 to 800 °C with a rate of 10 °C min^{-1} under air atmosphere. The air flow rate was controlled at 100 ml/min.

2.3. Catalytic tests

The catalytic experiments were performed in a continuous fixed-bed reactor (i.d. = 15 mm; length = 700 mm) which was placed in an electric furnace consisting of four heating zones equipped with four temperature controllers. The thermocouple was placed in the center of the catalyst bed to measure the temperature in the catalyst zone. The benzyl alcohol with a rate of 0.05 ml/min was pumped into the reactor by a syringe pump, and the flow of ammonia was controlled by a PID cascade controller to keep the flow rate as required. In the experiment, 15 ml of the catalyst sample was charged into the middle section of the reactor to create a catalyst zone of approximately 85 mm, and the catalyst zone was heated to the desired temperature. Controlled flows of benzyl alcohol and ammonia were passed separately into a vaporizer (approximately 205 °C) in which the two reactants were preheated, vaporized and mixed perfectly. The products were collected in a condenser, then the liquid products were separated in a gas-liquid separator, and the gaseous products generated were absorbed by passing through a flask filled with a solution of sulfuric acid to remove the low boiling point compounds and unreacted ammonia. A GC–MS (HP5971 GC–MS) equipped with a 30 m SE-30 capillary column was used to identify the collected products.

The products were analyzed quantitatively by a gas chromatograph equipped with a 30 m SE-30 capillary column. The selectivity of each liquid product was calculated using the calibration curves with 2, 6-lutidine as an internal standard. The GC temperature program was 140 °C for 10 min and 40 °C/min up to 220 °C.

3. Results and discussion

3.1. Catalyst selection

The purpose of this work was to convert benzyl alcohol to benzonitrile over a catalyst through the amination-dehydrogenation approach. Because $Co_{19.9}Ni_{3.0}/\gamma\text{-}Al_2O_3$ catalyst proved to be efficient in the conversion of ethanol to acetonitrile [23,27,28], we initially run the reaction of benzyl alcohol to benzonitrile over this catalyst. However, low selectivity towards benzonitrile was achieved. It has been disclosed that the conversion of aliphatic alcohols to the corresponding nitriles over $Co_{19.9}Ni_{3.0}/\gamma\text{-}Al_2O_3$ catalyst involves three elementary steps, which are dehydrogenation of alcohols to their corresponding aldehydes, condensation of aldehydes with ammonia to imines, and dehydrogenation of imines to nitriles [23,27,28]. In addition to being a support, $\gamma\text{-}Al_2O_3$ also acts as an acid to promote the condensation of aldehydes with ammonia to form imines; and the transition metals are the dehydrogenation active components in the catalyst. It is in this context that we began to prepare a series of catalysts from various supports and transition metals to obtain a catalyst with good performance in the conversion of benzyl alcohol to benzonitrile. Because copper was mostly reported to be active in the dehydrogenation of imines, amines and alcohols [32,33], a series of catalysts with different copper contents doped on to SiO_2 were prepared firstly. Their catalysis in the reaction was evaluated and the results are listed in Table 1. As shown in Table 1, neat SiO_2 had no activity in the reaction (Table 1, entry 1). All the catalysts showed very high activity in view of the benzyl alcohol conversion, but the selectivity towards benzonitrile changed with the copper content. At 5.1% of copper content, the conversion of benzyl alcohol was 92.2%, and the selectivity towards benzonitrile was 74.0%. In addition to benzonitrile, dibenzylamine and tribenzylamine which are direct amination products were formed in selectivity of 12.5% and 3.8%. When the copper content increased from 5.1 to 10.3%, both the conversion of benzyl alcohol and the selectivity towards benzonitrile increased, and the selectivity towards dibenzylamine and tribenzylamine decreased (Table 1, entries 2, 3). These results indicate that increasing copper content enhanced the dehydrogenation capacity of the catalyst. However, when the copper content was higher than 10.3%, the selectivity towards benzonitrile decreased with further increase of the copper content due to the formation of benzene and methylbenzene (Table 1, entries 4, 5). When the copper content was 24.9%, the conversion of benzyl alcohol was still close to 100%, however, the selectivity towards benzonitrile began to decrease (Table 1, entry 6), which may be ascribed to the copper agglomeration at overly high copper content, decreasing the dehydrogenation activity of the catalyst. From above experimental results it can be seen that $Cu_{10.3}/SiO_2$ had good performance compared to the other catalysts investigated.

Next, several catalysts from 10% of copper doped on to $\gamma\text{-}Al_2O_3$, H-ZSM-5, ZrO_2, TiO_2, mordenite, $CaCO_3$ and sodium bentonite were prepared. Their catalytic performances in the reaction were assessed, and the results are shown in Table 2 (Table 2, entries 1–8). From Table 2 it can be seen that the catalytic performances of the catalysts varied with the support, though the doped copper are present in CuO crystallites in all the catalysts (Fig. S1). Among all the catalysts $Cu_{10.3}/SiO_2$ was the best one under the same reaction conditions. The benzyl alcohol conversion over this catalyst was 99%, and the selectivity of benzonitrile was higher than 89% under atmospheric ammonia pressure at 320 °C. Catalyst $Cu_{10.3}$/sodium bentonite also showed good performance from the view points of the conversion of benzyl alcohol and the selectivity of benzonitrile in the first 2 h on stream, but it deactivated quickly after then. This can be ascribed to the quick loss of its acidity during the catalytic run, which was disclosed by the IR spectra of adsorbed pyridine (Fig. S2). $Cu_{10.4}/CaCO_3$ showed the worst results among all the catalysts screened, both the conversion of benzyl alcohol and the selectivity towards benzontrile were low and the main product was benzaldehyde. The IR spectra of adsorbed pyridine revealed that both the fresh and used samples of $Cu_{10.4}/CaCO_3$ have very low acidity (Fig. S2). $Cu_{10.1}/TiO_2$ and $Cu_{10.3}/ZrO_2$ also showed high activity in the conversion of benzyl alcohol to benzonitrile. However, the selectivity towards benzonitrile over $Cu_{10.1}/TiO_2$ and $Cu_{10.3}/ZrO_2$ was lower compared to that over $Cu_{10.3}/SiO_2$. These could be ascribed to the higher selectivities of toluene and benzylamine over $Cu_{10.1}/TiO_2$ and $Cu_{10.3}/ZrO_2$ respectively under the same reaction conditions (Table 2, entries 7, 8). Because SiO_2 is the best one among all the selected inorganic supports, several other catalysts from SiO_2 doping with about 10% of iron, cobalt, nickel, zinc and chromium were then prepared respectively due to their activities in the dehydrogenation of imines to nitriles [23,27,28,30]. Their performances on the reaction were evaluated too, and the results are also listed in Table 2. These catalysts showed poor catalytic results compared to $Cu_{10.3}/SiO_2$ (Table 2, entries 9–13). Especially in the cases of Ni and Cr as the doped metals, the conversion of benzyl alcohol was lower than 5% (Table 2, entries 9, 12). The IR spectra of adsorbed pyridine disclosed that both $Ni_{10.2}/SiO_2$ and $Cr_{10.2}/SiO_2$ have very low acidity compared to $Ni_{10.2}/SiO_2$ (Fig. S3). Besides, NiO and Cr_2O_3 crystalline phases were identified by XRD in $Ni_{10.2}/SiO_2$ and $Cr_{10.2}/SiO_2$ respectively, and these crystalline phases were maintained in the used samples (Fig. S4, S5). Therefore, the low acidity and the weak dehydrogenation capacities of NiO and Cr_2O_3 crystallites might be the reasons that both $Ni_{10.2}/SiO_2$ and $Cr_{10.2}/SiO_2$ performed very poorly in the conversion of benzyl alcohol to benzontrile. Based on the above results it can be concluded that the performance of a catalyst in the conversion of benzyl alcohol to benzonitrile is determined by both the support and the metal doped. $Cu_{10.3}/SiO_2$ performed best in all the prepared catalysts.

3.2. Performance of the $Cu_{10.3}/SiO_2$ catalyst under different reaction conditions

The influence of the reaction temperature on the performance of the $Cu_{10.3}/SiO_2$ catalyst was investigated in the temperature range of 290–400 °C under atmospheric ammonia pressure, molar ratio of ammonia to benzyl alcohol of 10:1 and GHSV of 178 h^{-1}. The results shown in Table 3 indicated that the conversion of benzyl alcohol was close to 100% in the investigated temperature range. The selectivity towards benzonitrile increased with the temperature increase from 290 °C to 340 °C (Table 3, entries 1–6). The selectivity towards benzonitrile reached its maximum of 95.9%, at 340 °C (Table 3, entry 6). Above that temperature, the selectivity decreased with further increase of the temperature. Overly high reaction temperature, for instance 400 °C, led to more benzyl alcohol hydrogenation to toluene (Table 3, entry 10), and decomposition to gaseous molecules and carbonous compound deposition on the catalyst.

The influence of the molar ratio of ammonia to benzyl alcohol on the reaction was first investigated under atmospheric ammonia pressure and GHSV of 178 h^{-1} at 340 °C. The results are presented in Table 4. As shown in the table, the conversion of benzyl alcohol was close to 100% under all investigated molar ratios of ammonia to benzyl alcohol, and the selectivity towards to benzonitrile increased with an increase in the molar ratio of ammonia to ben-

Table 1
Effect of copper content on the performances of the catalysts on the conversion of benzyl alcohol to benzonitrile.

Entry	Catalyst	Conversion (%)	Selectivity (%)						Carbon balance (%)
			Ben	Tol	Bal	Benn	Dba	Tba	
1	SiO_2	0	0	0	0	0	0	0	
2	$Cu_{5.1}/SiO_2$	92.2	0	0.7	0.9	74.0	12.5	3.8	93.5
3	$Cu_{10.3}/SiO_2$	99.4	0.1	0.5	3.3	89.9	1.5	1.1	95.3
4	$Cu_{14.9}/SiO_2$	99.1	0.9	1.5	3.4	86.3	0.6	0.2	94.0
5	$Cu_{20.1}/SiO_2$	99.2	0.9	1.4	3.3	85.7	1.6	1.1	94.4
6	$Cu_{24.9}/SiO_2$	98.8	0.9	1.4	3.4	83.0	1.6	1.1	92.5

Ben: Benzene, Tol: Toluene, Bal: Benzaldehyde, Benn: Benzonitrile, Bena: Benzylamine, Dba: Dibenzylamine, Tba: Tribenzylamine.
Reaction conditions: catalyst dosage 15 ml, reaction temperature 320 °C, atmospheric pressure, ammonia/benzyl alcohol molar ratio 10:1, GHSV 178 h^{-1}, time on stream 2 h.

Table 2
Performance of the prepared catalysts on the conversion of benzyl alcohol to benzonitrile.

Entry	Catalyst	Conversion(%)	Selectivity (%)								Carbon balance (%)
			Ben	Tol	Bal	Benn	Dbe	Bena	Dba	Tba	
1	$Cu_{10.3}/SiO_2$	99.4	0.1	0.5	3.3	89.9	0	0	1.5	1.1	95.3
2	$Cu_{10.2}/\gamma$-Al_2O_3	98.6	0	5.8	4.3	70.2	11.4	0	1.4	0.9	94.2
3	$Cu_{10.2}$/mordenite	97.9	0	2.2	2.2	70.9	11.6	0	5.5	2.2	95.7
4	$Cu_{9.9}$/HZSM-5	98.6	0.2	8.1	0	62.9	12.1	0	7.8	3.5	94.0
5	$Cu_{10.3}$/sodium bentonite	97.4	0.1	1.3	2.2	87.2	0	0	2.3	1.2	94.5
6	$Cu_{10.4}/CaCO_3$	66.3	0.4	1.2	46.4	37.0	0	0	5.0	2.6	93.6
7	$Cu_{10.1}/TiO_2$	97.4	0	13.4	0.1	77.7	0	0	0.4	0.5	94.2
8	$Cu_{10.3}/ZrO_2$	98.2	0	2.2	0	74.6	0	18.0	0	0	95.3
9	$Ni_{10.2}/SiO_2$	4.3	1.1	3.8	12.8	28.8	0	0	49.5	0	95.5
10	$Fe_{10.3}/SiO_2$	72.6	0	15.9	5.5	5.0	1.4	0	6.3	26.5	67.6
11	$Zn_{10.0}/SiO_2$	55.7	0	5.3	0	2.2	5.7	1.3	10.9	50.1	85.6
12	$Cr_{10.3}/SiO_2$	4.0	0	9.8	12.9	14.9	0	0	62.8	0	97.3
13	$Co_{9.9}/SiO_2$	24.8	2.2	3.3	1.7	26.2	0	0	46.7	18.1	98.3

Ben: Benzene, Tol: Toluene, Bal: Benzaldehyde, Benn: Benzonitrile, Dbe: Dibenzylether, Bena: Benzylamine, Dba: Dibenzylamine, Tba: Tribenzylamine.
Reaction conditions: catalyst dosage 15 ml, reaction temperature 320 °C, atmospheric pressure, ammonia/benzyl alcohol molar ratio 10:1, GHSV 178 h^{-1}, time on stream 2 h.

Table 3
Effect of the temperature on the performance of the $Cu_{10.3}/SiO_2$ catalyst.

Entry	Temperature (°C)	Conversion (%)	Selectivity (%)						Carbon balance (%)
			Ben	Tol	Bal	Benn	Dba	Tba	
1	290	97.6	0.4	0.5	5.6	78.1	4.2	3.1	92.1
2	300	99.1	0.2	0.5	4.4	84.2	3.2	2.8	93.0
3	310	99.1	0.1	0.4	4.1	89.7	1.6	1.1	93.2
4	320	99.2	0.1	0.5	3.3	89.9	1.5	1.1	95.3
5	330	99.3	0.3	0.6	0.8	94.7	1.8	1.2	96.1
6	340	99.4	0.2	0.3	0.4	95.9	0.6	0	98.3
7	350	99.4	0.1	0.8	0	95.4	0.7	0	97.3
8	360	99.8	0.1	1.0	0	94.9	1.6	1.1	95.9
9	380	99.9	0.4	2.1	0.5	89.7	1.6	1.4	94.4
10	400	100	0.4	3.5	1.9	84.1	1.7	1.9	93.5

Ben: Benzene, Tol: Toluene, Bal: Benzaldehyde, Benn: Benzonitrile, Bena: Benzylamine, Dba: Dibenzylamine, Tba: Tribenzylamine.
Reaction conditions: atmospheric pressure, ammonia/benzyl alcohol molar ratio 10:1, GHSV 178 h^{-1}, time on stream 2 h.

Table 4
Effect of molar ratio of ammonia to benzyl alcohol on the performance of the $Cu_{10.3}/SiO_2$ catalyst.

Entry	n_A/n_B	GHSV (h^{-1})	Conversion (%)	Selectivity (%)						Carbon balance (%)
				Ben	Tol	Bal	Benn	Dba	Tba	
1	12:1	178	99.4	0.1	0.2	0.3	95.2	0.3	0	96.4
2	11:1	178	99.4	0.1	0.3	0.3	95.8	0.3	0	97.3
3	10:1	178	99.4	0.2	0.3	0.4	95.9	0.4	0	97.7
4	9:1	178	99.2	0.5	0.5	0.7	95.5	0.6	0	97.8
5	8:1	178	99.3	0.6	0.6	1.4	95.4	0.7	0	98.7
6	6:1	178	99.3	0.6	0.8	1.7	94.4	1.0	0.2	98.8
7	4:1	178	99.1	1.1	1.1	2.4	91.4	1.4	0.6	98.3
8	10:1	445	100	0.1	0.5	0	98.0	0.7	0	99.3
9	8:1	445	99.1	0.6	0.6	0.4	95.6	0.7	0	98.1
10	6:1	445	99.1	0.6	0.8	0.7	93.6	1.0	0	96.7

n_A/n_B: Ammonia/Benzyl alcohol, Ben: Benzene, Tol: Toluene, Bal: Benzaldehyde, Benn: Benzonitrile, Bena: Benzylamine, Dba: Dibenzylamine, Tba: Tribenzylamine.
Reaction conditions: atmospheric pressure, reaction temperature 340 °C, time on stream 2 h.

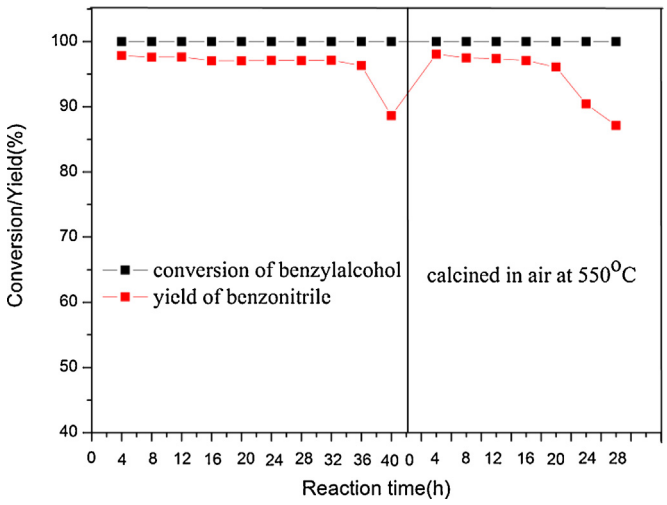

Fig. 1. The conversion benzyl alcohol and the yield of benzonitrile with reaction time.

zyl alcohol from 4:1 to 10:1 and reached its maximum of 95.9% at a molar ratio of 10:1 (Table 4, entry 3). The reason may be that appropriately excessive ammonia can suppress the formation of toluene, dibenzylamine and tribenzylamine, and promote the condensation of benzaldehyde to imine with ammonia. With further increases in the molar ratio of ammonia to benzyl alcohol the electivity towards to benzonitrile decreased slightly due to the formation of some unidentified compounds. After obtaining these results, the reaction was further investigated under GHSV of 445 h^{-1} at the molar ratio of ammonia to benzyl alcohol of 10:1, 8:1 and 6:1, respectively (Table 4, entries 8–10). It was revealed again that the highest yield of benzonitrile was achieved at the molar ratio of 10:1 (Table 4, entry 8).

The influence of GHSV on the catalytic performance of the catalyst was investigated under atmospheric ammonia pressure and a molar ratio of ammonia to benzyl alcohol of 10:1 at 340 °C. The results shown in Table 5 indicated that the conversion of benzyl alcohol was close to 100% in the GHSV range of 178 h^{-1} to 946 h^{-1}. With the decrease of GHSV from 946 h^{-1} to 445 h^{-1}, the selectivity towards benzonitrile increased from 93.1% to 98.0% (Table 5, entries 4–9). However, with further decrease of GHSV the selectivity towards benzonitrile decreased gradually.

From the investigation of parameter effects on the conversion of benzyl alcohol to benzonitrile, an optimized process for the synthesis of benzonitrile over the $Cu_{10.3}/SiO_2$ catalyst was obtained, which is running the reaction at 340 °C under atmospheric ammonia pressure while keeping the ammonia/alcohol molar ratio of 10:1 and GHSV of 445 h^{-1}, respectively. Under the optimized conditions the yield of benzonitrile reached 98.0% at the time that the catalyst was on stream for 2 h.

3.3. Lifetime and regeneration of the $Cu_{10.3}/SiO_2$ catalyst

The lifetime of the $Cu_{10.3}/SiO_2$ catalyst was investigated under the optimized conditions and the results are shown in Fig. 1. The conversion of benzyl alcohol was always close 100%; the selectivity towards benzonitrile was higher than 97% in the first 32 h, then it decreased gradually with the time that the catalyst was on stream. The selectivity of benzonitrile dropped from 98.0% to 88.6% after the catalyst was on stream for 40 h. The catalyst was regenerated by calcination in air for 6 h at 550 °C, then the reaction was carried out again using the regenerated catalyst. Both the conversion of benzyl alcohol and the selectivity towards benzonitrile over the regenerated catalyst are close to those over the fresh catalyst during the first 16 h. The lifetime of the regenerated catalyst was shorter than that of the fresh one. The reasons leading to the deactivation of the catalyst and deviation of the regenerated catalyst from the fresh one will be discussed in the characterization section.

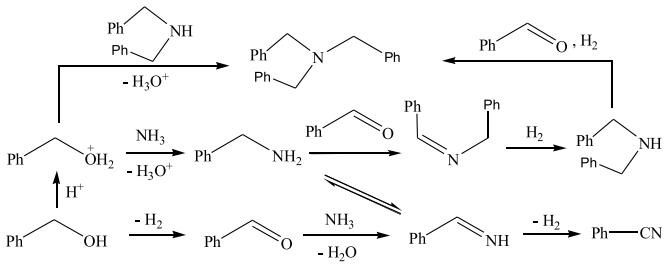

Scheme 1. Pathways for the formation of benzonitrile and main by-products.

3.4. Pathways for product generation

For screening the pathway of benzyl alcohol conversion to benzonitrile the reaction was run at a large GHSV of 2838 h^{-1} (Table 5, entry 10). The composition of the reaction mixture was analyzed by GC–MS. In this case, the conversion of benzyl alcohol was 89.5%, lower than those at low GHSV. Meanwhile, benzaldehyde with a selectivity of 16.1% was observed. Same as that acetaldehyde is an intermediates in the conversion of ethanol to acetonitrile [23,32], benzaldehyde is a key intermediate in the conversion of benzyl alcohol to benzonitrile. Besides, benzylamine, dibenzylamine and tribenzylamine as by-products were also detected. Taking into account the catalytic results shown in Table 5, the pathways proposed for the transformation of ethanol to acetonitrile [23,32], and synthesis of amines in literature [34–36], we are able to propose pathways for benzyl alcohol conversion to the products (Scheme 1).

During the catalytic conversion of benzyl alcohol, dehydrogenation occurred on the catalyst's active sites of hydrogenation-dehydrogenation, producing benzaldehyde and hydrogen. Benzaldehyde condensed with ammonia on the acid sites to generate the intermediate benzyleneimine, which was dehydrogenated to give benzonitrile. Meanwhile, amination of benzyl alcohol on the acid sites generate benzylamine, which immediately condensed with benzaldehyde to give the intermediate N-benzyl benzyleneimine or was transformed to benzyleneimine by dehydrogenation. N-benzyl benzyleneimine underwent hydrogenation to afford dibenzylamine. Two possible pathways might be present to form dibenzylamine. One is the direct amination of benzyl alcohol with dibenzylamine on the acid sites, and the other is reductive amination of benzaldehyde with dibenzylamine on the catalyst's active sites of hydrogenation-dehydrogenation.

3.5. Catalyst characterization

The catalysts were characterized by XRD, ICP, TEM-EDX, N_2 adsorption–desorption, and IR spectra of adsorbed pyridine. Fig. 2 shows the XRD patterns of samples of the catalysts. For all the samples, the peaks representing the support SiO_2 were observed. In addition, the XRD patterns of the fresh $Cu_{5.1}/SiO_2$, $Cu_{10.3}/SiO_2$, $Cu_{14.9}/SiO_2$ and $Cu_{24.9}/SiO_2$ exhibited peaks ascribed to CuO crystalline phase. And the peak strength increased with the increase of copper content in the catalysts, which indicated that high copper loading led to big size of CuO crystalline phase. However, a Cu crystalline phase, instead of CuO crystalline phase, was found in the patterns of the sample of used $Cu_{10.3}/SiO_2$. We supposed that CuO was reduced to Cu by in suit generated H_2 during the catalytic run as shown in Eq. (5) [37,38], and the real active species of dehydro-

Table 5
Effect of GHSV on the performance of the $Cu_{10.3}/SiO_2$ catalyst.

Entry	GHSV (h^{-1})	Conversion (%)	Selectivity (%)						Carbon balance (%)
			Ben	Tol	Bal	Benn	Dba	Tba	
1	178	99.4	0.2	0.3	0.4	95.9	0.6	0	97.5
2	267	100	0.1	0.6	0	96.2	1.8	0	98.8
3	356	100	0.1	0.5	0	96.9	1.2	0	98.7
4	445	100	0.1	0.5	0	98.0	0.7	0	99.3
5[a]	445	100	0.16	0.72	0	97.9	0.58	0	99.2
6	534	100	0.1	0.5	0	96.8	0.9	0	98.4
7	623	100	0.1	0.5	0	95.7	1.1	0	97.3
8	712	100	0.2	0.6	0.7	94.9	1.2	0	97.7
9	946	100	0.4	0.5	0.8	93.1	2.1	0	96.9
10	2838	89.5	0.3	0.4	16.1	71.9	1.6	2.2	92. 6

Ben: Benzene, Tol: Toluene, Bal: Benzaldehyde, Benn: Benzonitrile, Bena: Benzylamine, Dba: Dibenzylamine, Tba: Tribenzylamine.
Reaction conditions: atmospheric pressure, reaction temperature 340 °C, ammonia/benzyl alcohol molar ratio 10:1, time on stream 2 h.
[a] The catalyst was pre-reduced by H_2.

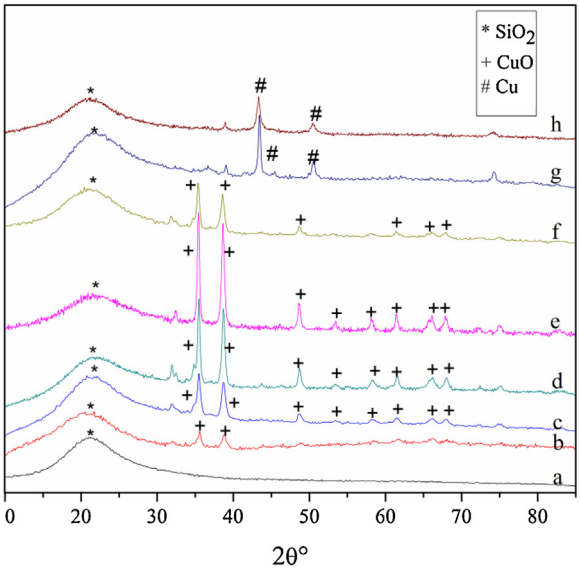

Fig. 2. XRD patterns of the catalyst samples. (a) SiO_2, (b) $Cu_{5.1}/SiO_2$, (c) $Cu_{10.3}/SiO_2$, (d) $Cu_{14.9}/SiO_2$, (e) $Cu_{24.9}/SiO_2$ (f) $Cu_{10.3}/SiO_2$ (regenerated), (g) $Cu_{10.3}/SiO_2$ (used), (h) $Cu_{10.3}/SiO_2$ (reduced).

Table 6
Textural properties of the SiO_2, the fresh, used and regenerated $Cu_{10.3}/SiO_2$.

Catalyst	S^a_{BET} ($m^2\,g^{-1}$)	V^b ($cm^3\,g^{-1}$)	$d_p{}^c$ (nm)
SiO_2	225	0.188	2.91
$Cu_{10.3}/SiO_2$ (fresh)	198	0.147	2.82
$Cu_{10.3}/SiO_2$ (used)	25	0.065	7.26
$Cu_{10.3}/SiO_2$ (regenerated)	193	0.114	2.77

[a] BET surface area.
[b] BJH cumulative desorption pore volume.
[c] BJH cumulative desorption mean pore diameter.

Table 7
The amount of pyridine adsorbed on the catalysts and the crystallites diameters of Cu species in the catalyst samples.

Catalyst sample	C[a] (mmol/g)	d[b] (nm)	
		CuO	Cu
$Cu_{5.1}/SiO_2$	228.06	13.7	–
$Cu_{10.3}/SiO_2$ (fresh)	287.36	16.3	–
$Cu_{10.3}/SiO_2$ (regenerated)	262.28	–	26.0
$Cu_{10.3}/SiO_2$ (used)	230.55	20.2	–
$Cu_{24.9}/SiO_2$	362.34	24.3	–

[a] The amount of pyridine adsorption per gram of catalyst.
[b] The crystallites diameters of Cu species calculated using Scherrer equation from the XRD patterns.

genation in the conversion of benzyl alcohol to benzonitrile might be Cu.

$$CuO + H_2 \rightarrow Cu + H_2O \quad (5)$$

To confirm this inference, fresh $Cu_{10.3}/SiO_2$ was placed on hydrogenation stream at 340 °C for 2 h to reduce CuO to Cu. The XRD patterns of the reduced sample were almost same as those of the used one (Fig. 2g and h). And the reduced catalyst demonstrated almost same catalytic performance as that of the fresh $Cu_{10.3}/SiO_2$ (Table 5, entries 4, 5). These results support the supposition above.

In the patterns of the sample of the regenerated $Cu_{10.3}/SiO_2$, no peaks representing the Cu crystalline phase were observed, instead, the peaks representing CuO crystalline phase appeared again, indicating that Cu was converted to CuO through calcination at 550 °C for 6 h (Table 6).

The crystallites diameters of Cu species in the fresh, used and regenerated $Cu_{10.3}/SiO_2$ were calculated by using Scherrer formula and the results are summarized in Table 7. The average diameters of the CuO crystallites in the fresh and regenerated samples of the $Cu_{10.3}/SiO_2$ catalyst were calculated to be 16.3 nm and 20.2 nm, respectively. Besides, the average diameter of Cu crystallites in the sample of the used catalyst was 26.0 nm. The changing in diameter of the CuO crystallites indicated that CuO was sintered during the catalytic process. Therefore, we can conclude that the sintering of CuO might be one reason that the performance of the regenerated catalyst deviated from that of the fresh one (Fig. 1). On the other hand, the average diameter of the CuO crystallites in the regenerated sample is smaller than that of Cu crystallites in the used sample. This is due to the redispersion of the active phase during oxidation treatment of the sample in air at 550 °C, which is a common phenomenon in the regeneration of Cu/SiO_2 catalysts [39].

The specific surface areas and porous structure of the SiO_2, the fresh, used, and regenerated $Cu_{10.3}/SiO_2$ were analyzed by N_2 adsorption-desorption. The adsorption-desorption isotherms are shown in Fig. 3. Except for the used one, all of the other samples exhibited a type IV Langmuir isotherm according to the IUPAC classification, which indicated the existence of mesopores in the catalysts. The sample of the used catalyst exhibited a type I Langmuir isotherm, which indicated the existence of micropores in the catalyst. The results revealed that some substances deposited in the pores of the catalyst during the catalytic run.

Table 6 summarizes textural properties of the SiO_2, the fresh, used, and regenerated $Cu_{10.3}/SiO_2$. The fresh $Cu_{10.3}/SiO_2$ catalyst showed a slightly lower surface area compared to the SiO_2, and the pore volume decreased from 0.188 cm^3g^{-1} to 0.147 cm^3g^{-1}, indicating deposition of CuO crystalites in the pores of the SiO_2. Compared to the fresh catalyst, the used catalyst exhibited a sharp

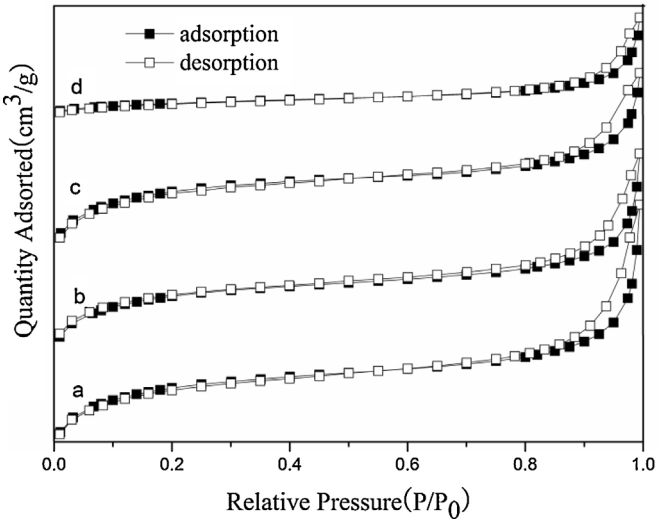

Fig. 3. Adsorption-desorption isotherms of catalyst samples. (a) SiO_2, (b) $Cu_{10.3}/SiO_2$ (fresh), (c) $Cu_{10.3}/SiO_2$ (regenerated), (d) $Cu_{10.3}/SiO_2$ (used).

decrease of surface area in combination with a big decrease of pore volume and a big increase of pore diameter. The drop in the pore volume could be the result of the deposition of a certain amount of carbon and other nonvolatile materials in the pores of the catalyst during the catalytic run. Table 6 also shows that the regenerated catalyst had a slightly lower surface area and pore volume than those of the fresh one, which can be ascribed to the fact that the CuO was partly sintered during the catalytic run and regeneration process. This can be confirmed by XRD and TEM investigations. Besides, the mean pore diameter of the used catalyst increased largely compared to that of the fresh catalyst, which can be attributed to that the pores with small diameters were blocked due to the deposition of carbon and other non-volatile materials.

Fig. 4 shows the TEM images of the samples of the fresh, used and regenerated $Cu_{10.3}/SiO_2$ catalyst. The TEM image of the sample of the fresh catalyst revealed that CuO particles well dispersed on the surface of the pores. After catalytic run, the CuO or Cu particles sintered. The particle sizes of the fresh, used, regenerated $Cu_{10.3}/SiO_2$ samples are located about 5 nm, 10–15 nm and 7–12 nm, respectively. The diameter changing trend revealed by the TEM is in line with that disclosed by XRD. The sintering of CuO crystallites might be one reason that the performance of the regenerated catalyst deviated from that of the fresh catalyst. It was found that amorphous substances covered on the surface of the catalyst by comparing the image of the used catalyst with that of the fresh one, which led to the CuO particles were not clearly displayed. This was supported by the EDX analysis (Fig. 4d). The carbon contents are 10.3%, 16.6%, and 11.2% at the points 1, 2 and 3, respectively. The TEM and EDX analysis results indicated that the deactivation of the catalyst was mainly caused by carbon deposition.

Fig. 5 shows the TGA-DSC plots of the samples of the fresh, used and regenerated $Cu_{10.3}/SiO_2$ catalyst. The fresh and regenerated samples respectively show an endothermic stage in the temperature range of 25–200 °C and 25–100 °C, with a weight loss of about 3% and 3.3%, attributed to desorption of physisorbed water and other small molecules. The used sample exhibits one slow weight loss of about 3% in the temperature range of 25–350 °C without obvious endothermic process, and another weight loss of about 5%

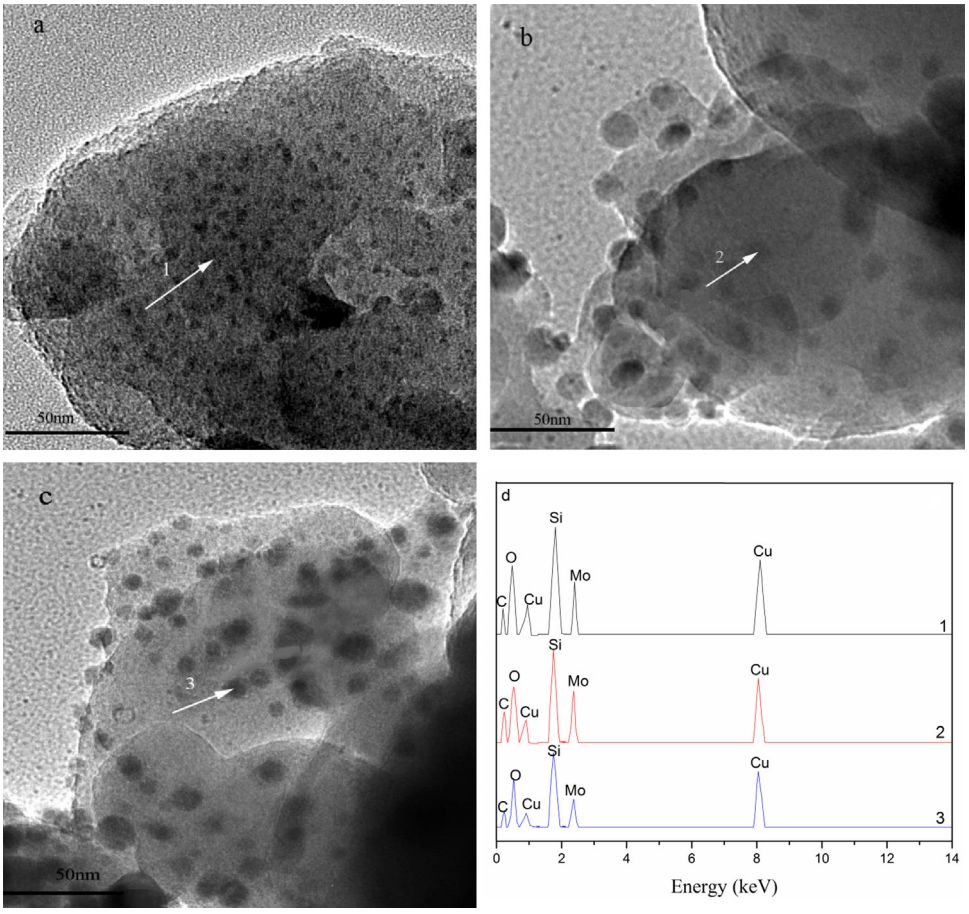

Fig. 4. TEM images of the catalyst samples and EDX spectra at points 1, 2 and 3. (a) $Cu_{10.3}/SiO_2$ (fresh), (b) $Cu_{10.3}/SiO_2$ (used), (c) $Cu_{10.3}/SiO_2$ (regenerated).

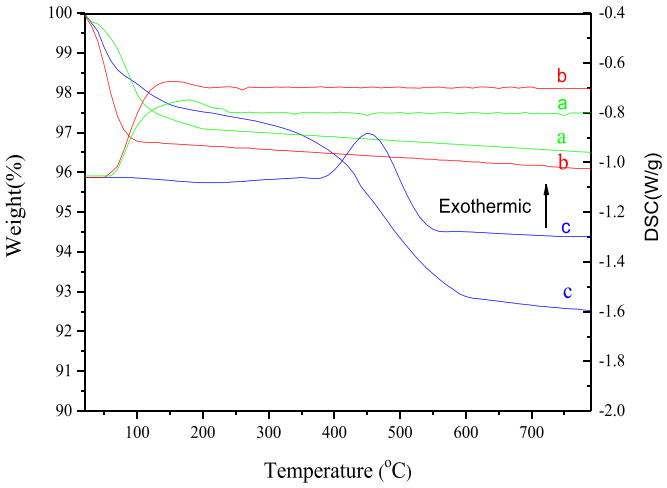

Fig. 5. TG-DSC analysis of the fresh, used and regenerated $Cu_{10.3}/SiO_2$ catalyst. (a) $Cu_{10.3}/SiO_2$ (fresh), (b) $Cu_{10.3}/SiO_2$ (regenerated), (c) $Cu_{10.3}/SiO_2$ (used).

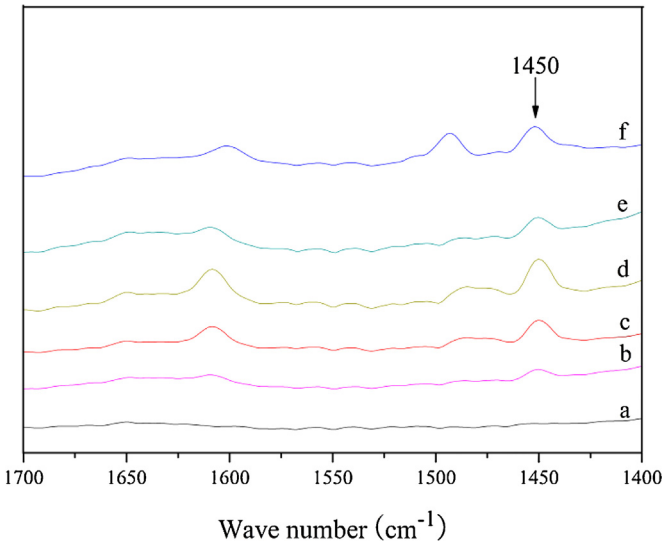

Fig. 6. IR spectra of pyridine adsorbed on the catalysts. (a) SiO_2, (b) $Cu_{5.1}/SiO_2$, (c) $Cu_{10.3}/SiO_2$(fresh), (d) $Cu_{24.9}/SiO_2$, (e) $Cu_{10.3}/SiO_2$(regenerated), (f) $Cu_{10.3}/SiO_2$(used).

between 200 and 600 °C with strong exothermic process due to the combustion of carbonaceous deposits. The difference of TGA and DSC plots among the samples indicates that carbonaceous compounds deposited on the pores of the catalyst during the catalytic run, and the carbonaceous deposits can be removed by combustion.

Fig. 6 shows the IR spectra of absorbed pyridine of the SiO_2, $Cu_{5.1}/SiO_2$, $Cu_{10.3}/SiO_2$, $Cu_{24.9}/SiO_2$, used $Cu_{10.3}/SiO_2$ and regenerated $Cu_{10.3}/SiO_2$ samples in the region 1700–1400 cm^{-1}. Generally, two peaks at 1545 cm^{-1} and 1450 cm^{-1} ascribed to the characteristic absorptions of pyridine adsorbed on the Brønsted and Lewis acid centers respectively are observed if both the acid sites are present in a catalyst [40–42]. Neither peak appeared in the spectrum of SiO_2, indicating that neat SiO_2 has no acidity. Therefore, no conversion of benzyl alcohol to benzonitrile was observed over neat SiO_2 (Table 1, entry 13), because the acid centers provide the catalyst with the ability to catalyze the condensation of benzaldehyde with ammonia to benzyleneimine. The doping of copper into SiO_2 only created Lewis acid centers on the matrix of SiO_2 because only a peak at 1450 cm^{-1} was observed in the spectra of the catalysts (Fig. 6). The quantification of the amount of acid sites of the catalyst samples determined by the IR spectra of absorbed pyridine is given in Table 7. From the table we can see that the Lewis acidity of the catalyst increased with the doping amount of copper. Because the condensation reaction took place over the Lewis acid centers in the catalyst, high doping amount of copper was in favor of the condensation. However, the yield of benzonitrile was not in proportion to the acidity of the catalysts. $Cu_{10.3}/SiO_2$ performed best among all the catalysts, which indicated that acidity of the catalyst is not the sole factor in determining the catalysis of the catalyst. The sizes of the CuO particles and the surface areas of the catalysts are also important factors in determining the performance of the catalysts. In fact, over-doping of copper led to big sizes of the CuO particles (Table 7), and small surface areas of the catalysts, which were detrimental to the dehydrogenation of benzyl alcohol and intermediate benzyleneimine (Scheme 1), and the overall reaction. Therefore, the $Cu_{24.9}/SiO_2$ performed worse compared to $Cu_{10.3}/SiO_2$ in the conversion of benzyl alcohol to benzonitrile, though its acidity is higher than that of $Cu_{10.3}/SiO_2$.

The spectrum of the used $Cu_{10.3}/SiO_2$ catalyst is different from that of the fresh one. Besides the peak at 1450 cm^{-1} an additional peak around 1495 cm^{-1} was observed, which indicated that some substances deposited on the surface of the catalyst in the catalytic run. This peak disappeared in the spectrum of the regenerated catalyst and the strength of the peak at 1450 cm^{-1} was weaker in some degree than that in the spectrum of the fresh catalyst. From Table 7 we can clearly find that the amount of acid sites of the used sample decreased compared to that of the fresh one. After regeneration, the acidity of the catalyst increased but did not reach the value of the fresh one, and the sizes of the CuO particles were larger than those in the fresh one. These results indicate that sintering of copper particles during the catalytic run not only reduced the active sites of dehydrogenation, but also decreased the acidity of the catalyst. Therefore, the performance of the regenerated catalyst deviated from that of the fresh one.

Finally, the copper contents of the samples of the fresh and regenerated catalyst were 10.3% and 10.2% respectively. The content of copper almost maintained constant, which indicated that deviation of the performance of the regenerated catalyst from that of the fresh one was not caused by the leaking of copper during the catalytic run.

4. Conclusions

A $Cu_{10.3}/SiO_2$ catalyst was prepared, which showed activity for the conversion of benzyl alcohol to benzonitrile through amination-dehydrogenation process. The parameters that affected the catalyst performance were investigated carefully, and an optimized process for synthesizing benzonitrile from benzyl alcohol and ammonia over $Cu_{10.3}/SiO_2$ catalyst was obtained. Under the optimized conditions, the yield of benzonitrile reached 98.0%. The characterization results indicated that the doping of copper created Lewis acid sites in the matrix of SiO_2, which were the active centers of condensation reaction involved in the conversion of benzyl alcohol to benzonitrile. The doped copper in the fresh catalyst was present in CuO state, which was reduced to elemental Cu by H_2 generated in situ in the catalytic run. Elemental Cu was the real active species for the amination–hydrogenation process in the synthesis of benzonitrile. The characterization results also disclosed that the catalyst deactivation was mainly caused by the carbonaceous deposition on the surface of the catalyst in the catalytic reaction. The experimental results confirmed that most activity of the catalyst can be recovered at 550 °C online by blowing air into the reactor. The partial sintering of copper particles and the slight decrease of Lewis acidity caused by the sintering of copper particles, were the main causes that the performance of the regenerated $Cu_{10.3}/SiO_2$ catalyst deviated from that of the fresh one.

Acknowledgments

We thank the financial support of the National Natural Science Foundation of China (Grant No. 21476057), the Natural Science Foundation of Hebei Province of China (Grant No. B2015202284) and the Program for the Top Young Innovative Talents of Hebei Province of China.

Appendix A. Supplementary data

Supplementary data associated with this article can be found, in the online version, at http://dx.doi.org/10.1016/j.apcata.2016.04.031.

References

[1] M.A. Palafox, V.K. Rastogi, L. Mittal, J. Quantum Chem. 94 (2003) 189–204.
[2] T.D. Ros, M. Prato, D.M. Guldi, M. Ruzzi, L. Pasimeni, Chem A Eur. J. 7 (2001) 816–827.
[3] T. Konishi, M. Fujitsuka, O. Ito, Y. Toba, Y. Usui, Bull. Chem. Soc. Jpn. 74 (2001) 39–45.
[4] S. Komamine, M. Fujitsuka, O. Ito, A. Itaya, J. Photochem. Photobiol. A: Chem. 135 (2000) 111–117.
[5] A. Latini, F.K. Aldibaja, C. Cavallo, D. Gozzi, J. Power Sources 269 (2014) 308–316.
[6] A. Latini, R. Panetta, C. Cavallo, D. Gozzi, S. Quaranta, J. Nanomater. 2015 (2015), http://dx.doi.org/10.1155/2015/450405 (Article ID 450405, 8 pages).
[7] H.A.J. Carless, Y. Dove, Tetrahedron: Asymmetry 7 (1996) 649–652.
[8] F.de C. Pereira, B.A.V. Lima, A.P.de Lima, W.C. Pires, T. Monteiro, L.F. Magalhães, W. Costa, A.E. Graminha, A.A. Batista, J. Ellena, E.de P. Siveira-Lacerda, J. Inorg. Biochem. 149 (2015) 91–101.
[9] R.G. Rizayev, E.A. Mamedov, V.P. Vislovskii, V.E. Sheinin, Appl. Catal. A: Gen. 83 (1992) 103–140.
[10] E. Rombi, I. Ferino, R. Monaci, C. Picciau, V. Solinas, R. Buzzoni, Appl. Catal. A: Gen. 266 (2004) 73–79.
[11] T. Ishida, H. Watanabe, T. Takei, A. Hamasaki, M. Tokunaga, M. Haruta, Appl. Catal. A: Gen. 425–426 (2012) 85–90.
[12] M.K. Younes, A. Ghorbel, Appl. Catal. A: Gen. 197 (2000) 269–277.
[13] H. Berndt, K. Bilker, A. Martin, S. Rabe, Y. Zhang, M. Meisel, Catal. Today 32 (1996) 285–290.
[14] A. Martin, V.N. Kalevaru, B. Lücke, Catal. Today 78 (2003) 311–317.
[15] P. Nagaraju, Ch. Srilakshmi, N. Pasha, N. Lingaiah, I. Suryanarayana, P.S.S. Prasad, Catal. Today 131 (2008) 393–401.
[16] G.E. Gaumer, L. Jackson, Production of benzonitrile, to The Dow Chem. Comp. (1959) U.S. Patent 2872475.
[17] W.L. Fierce, C., Lake, W.J. Sandner, Process for the production of benzonitrile and phthalonitriles, to The Pure Oil Comp. (1961) U.S. Patent 2982780.
[18] T. Sandmeyer, Ber. Dtsch. Chem. Ges. 17 (1884) 1633–1635.
[19] C. Galli, Chem. Rev. 88 (1988) 765–792.
[20] K.W. Rosenmund, E. Struck, Ber. Dtsch. Chem. Ges. 52 (1919) 1749–1756.
[21] Q. Wen, J. Jin, L. Zhang, Y. Luo, P. Lu, Y. Wang, Tetrahedron Lett. 55 (2014) 1271–1280.
[22] C.J. Roger, S.J. Lawrence, J. Org. Chem. 46 (1981) 754–757.
[23] Y. Zhang, Y. Zhang, C. Feng, C. Qiu, Y. Wen, J. Zhao, Catal. Commun. 10 (2009) 1454–1458.
[24] C. Hamill, H. Driss, A. Goguet, R. Burch, L. Petrov, M. Daous, D. Rooney, Appl. Catal. A: Gen. 506 (2015) 261–267.
[25] B.M. Reddy, B. Manchar, J. Chem. Soc., Chem. Commun. 3 (1993) 234–235.
[26] S.J. Kulkarni, R. Ramachandra, J. Chem. Soc., Chem. Commun. 3 (1994) 273–283.
[27] D. Zhang, Y. Zhang, Y. Wen, K. Hou, J. Zhao, Chem. Eng. Res. Des. 89 (2011) 2147–2152.
[28] C. Feng, Y. Zhang, Y. Zhang, Y. Wen, J. Zhao, Catal. Lett. 141 (2011) 168–177.
[29] C. Feng, F. Guo, Y. Zhang, J. Zhao, Fine Chem. 27 (2010) 567–578 (in Chinese).
[30] Y. Zhang, W. Xu, J. Zhao, RSC Adv. 2 (2012) 6590–6598.
[31] Y. Zhang, T. Wei, Y. Pian, J. Zhao, Appl. Catal. A: Gen. 467 (2013) 154–162.
[32] Y. Hu, S. Jin, Z. Zhang, L. Zhang, J. Deng, H. Zhang, Catal. Commun. 54 (2014) 45–49.
[33] D. Damodara, R. Arundhathi, P.R. Likhar, Adv. Synth. Catal. 356 (2014) 189–198.
[34] B. Nişnci, K. Ganjehyan, Ö. Metin, A. Daştan, B. Török, J. Mol. Catal. A: Chem. 409 (2015) 191–197.
[35] A. Peeters, L. Claes, I. Geukens, I. Stassen, D.D. Vos, Appl. Catal. A: Gen. 469 (2014) 191–197.
[36] M. Ousmane, G. Perrussel, Z. Yan, J.M. Clacens, F.D. Campo, M. Pera-Titus, J. Catal. 309 (2014) 439–452.
[37] B. Zhang, S. Hui, S. Zhang, Y. Ji, W. Li, D. Fang, J. Nat. Gas Chem. 21 (2012) 563–570.
[38] S. Wang, X. Li, Q. Yin, L. Zhu, Z. Luo, Catal. Commun. 12 (2011) 1246–1250.
[39] A.J. Marchi, J.L.G. Fieero, J. Santamaría, A. Monzon, Appl. Catal. A: Gen. 142 (1996) 375–386.
[40] C.E. Volckmar, M. Bron, U. Bentrup, A. Martin, P. Claus, J. Catal. 261 (2009) 1–8.
[41] C.A. Emeis, J. Catal. 141 (1993) 347–354.
[42] E. Modrogan, M.H. Valkenberg, W.F. Hoelderich, J. Catal. 261 (2009) 177–187.